Available online at www.sciencedirect.com
SCIENCE DIRECT®
Journal of Organometallic Chemistry 689 (2004) 1821–1834
Journal of Organometallic Chemistry
www.elsevier.com/locate/jorganchem

Arene ruthenium complexes incorporating immine/azine hybrid-chelating N–N′ donor ligands: synthetic, spectral, structural aspects and DFT studies ☆

Anupam Singh [a], Manish Chandra [a], Abhaya N. Sahay [a], Daya S. Pandey [a,*], Krishna K. Pandey [b], Shaikh M. Mobin [c], M. Carmen Puerta [d], Pedro Valerga [d]

[a] *Department of Chemistry, Awadhesh Pratap Singh University, Rewa 486 003 (M.P), India*
[b] *School of Chemical Sciences, Devi Ahilya University, Indore 452 017 (M.P), India*
[c] *National Single Crystal X-ray Diffraction Laboratory, Indian Institute of Technology, Powai, India*
[d] *Departamento de Ciencia de los Materiales e Ingeniería Metalúrgica y Química Inorgánica, Facultad de Ciencias, Universidad de Cádiz, 11510 Puerto Real, Cádiz, Spain*

Received 8 January 2004; accepted 26 February 2004

Abstract

New series of mono and binuclear arene ruthenium complexes $[\{(\eta^6\text{-arene})RuCl(L)\}]^+$ and $[\{(\eta^6\text{-arene})RuCl\}_2(\mu\text{-L})_2]^{2+}$ (arene = benzene, *p*-cymene or hexamethylbenzene), {L = pyridine-2-carbaldehyde azine (paa), *p*-phenylene-bis(picoline)-aldimine (pbp) and *p*-bi-phenylene-bis(picoline)-aldimine (bbp)} are reported. The complexes have been fully characterized and molecular structure of the representative mononuclear complex $[(\eta^6\text{-}C_6Me_6)RuCl(paa)]BF_4$ (**1**), binuclear complexes $[\{(\eta^6\text{-}C_{10}H_{14})RuCl\}_2(\mu\text{-paa})](BF_4)_2$ (**3**) and $[\{(\eta^6\text{-}C_{10}H_{14})RuCl\}_2(\mu\text{-pbp})](BF_4)_2$ (**6**) have been determined by single crystal X-ray diffraction analyses. Single crystal X-ray structure determination revealed that in the binuclear complexes the $[(\eta^6\text{-}C_{10}H_{14})RuCl]^+$ units are *trans* disposed. Further, the crystal packing in the complexes **1**, **3** and **6** is stabilized by C–H···X type (X = Cl, F) inter, intramolecular hydrogen bonding and π–π stacking (**3**). To explore the ambiguous nature of the bonding between pyridine-2-carbaldehyde azine (paa) with ruthenium containing units $[(\eta^6\text{-arene})RuCl]^+$, DFT/B3LYP calculations have been performed on the complexes $[(\eta^6\text{-arene})RuCl(paa)]^+$ (arene = C_6H_6, **I**; C_6Me_6, **II**; $C_{10}H_{14}$, **III**).

Keywords: Ruthenium; Arene; Immine/azine; DFT; Single crystal X-ray structure

1. Introduction

There has been much interest towards synthesis, spectroscopic and electrochemical characterization of Ru(II) complexes with different polypyridyl and azo aromatic ligands. Such complexes have drawn immense interest due to their interesting photophysical and photochemical properties, potential use in several fields viz., photochemical molecular devices, in solar energy conversion, as light sensitive probes in biological systems and as photosensitizers in redox reactions [1]. Properties of the complexes largely depend upon the nature of the bridging ligand mediating metal–metal interactions. The specific role of bridging ligands is strongly influenced by the acceptor and donor properties of coordination sites, the length and rigidity of the spacers, the presence or absence of conjugated bonds, orientation of the substituents and scope of manipulating the ligand charge. In this regard, bridging poly-pyridyl ligands, viz. 2,2′-bipyrimidine (bpym); 2,3-bis(2-pyridyl)-pyrazine (bppz), 2,5-bis(2-pyridyl)-pyrazine, 3,5-bis(2-pyridyl)-1,2,4,5-tetrazine (bptz), azo-2,2′-bipyridine (abpy), 2,4,6-tris-! (2-pyridyl)-1,3,5-triazine, etc., have received considerable attention [2]. Closely related ligands having immine/azine hybrid-chelating systems viz., pyridine-

☆ Supplementary data associated with this article can be found, in the online version, at doi:10.1016/j.jorganchem.2004.02.037.

* Corresponding author. Tel.: +91766230684; fax: +91766230684.
E-mail address: dsprewa@yahoo.com (D.S. Pandey).

0022-328X/$ - see front matter © 2004 Elsevier B.V. All rights reserved.
doi:10.1016/j.jorganchem.2004.02.037

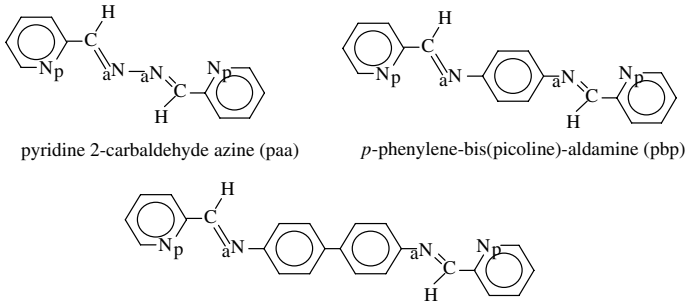

pyridine 2-carbaldehyde azine (paa)

p-phenylene-bis(picoline)-aldamine (pbp)

p-biphenylene-bis(picoline)-aldamine (bbp)

Scheme 1.

2-carbaldehyde azine (paa), *p*-phenylene-bis(picoline)-aldimine (pbp), *p*-biphenylene-bis(picoline)-aldimine (bbp) (Scheme 1) have relatively been less studied [3].

In general, these ligands possess low lying π^* orbital, which can back accept electron density from filled metal d_π orbital. As a consequence, they exhibit reversible reduction processes and intense charge transfer bands in the visible region. Among these, paa forms some unusual and rather interesting coordination compounds with the first series transition metal ions. The N_2 diazine linkage in the paa offers several possible mono and binucleating modes. Due to flexibility of the ligand around the N–N single bond it gives rise complexes having different geometries [4]. Reports dealing with structural data on the complexes resulting from interaction of paa with mainly 3d transition metal ions and a couple of 4d transition metal ions are available [3c,5a,5b]. Literature survey further indicated that, there are no reports dealing with the structural data on pbp or bbp complexes. Because of our interests in the development of *metallo-ligands or synthon* based on organometallic systems, we have made a detailed study on reactivity of the arene ruthenium complexes $[\{(\eta^6\text{-arene})RuCl(\mu\text{-}Cl)\}_2]$ (arene = benzene, *p*-cymene or hexamethylbenzene) with the ligands pyridine-2-carbaldehyde azine (paa), *p*-phenylene-bis-(picoline)-aldimine (pbp), *p*-biphenylene-bis(picoline)-aldimine (bbp) [6].

The reaction of hexamethylbenzene complex $[\{(\eta^6\text{-}C_6Me_6)RuCl(\mu\text{-}Cl)\}_2]$ with an excess of paa led to a mononuclear complex $[(\eta^6\text{-}C_6Me_6)RuCl(paa)]^+$. Our entire attempts to prepare mononuclear complexes containing pbp or bbp were unsuccessful at this stage (in the presence of excess of pbp or bbp). To better understand the nature of the bonding between paa with ruthenium containing units $[(\eta^6\text{-arene})RuCl]^+$, we have performed DFT/B3LYP calculations on the complexes $[(\eta^6\text{-arene})RuCl(paa)]^+$ (arene = C_6H_6, **I**; C_6Me_6, **II**; $C_{10}H_{14}$, **III**). The ligand paa forms both mono and binuclear complexes with transition metal systems. Many factors may affect the bonding modes of paa, such as ligand effects, charge on the complex and the replacement of one metal center by another. Concerning the nature of arene ligands, the interesting experimental observation is that the paa forms mononuclear complex $[(\eta^6\text{-}C_6Me_6)RuCl(paa)]^+$ when the arene ligand is hexamethylbenzene, whereas paa forms binuclear complex $[\{(\eta^6\text{-}C_{10}H_{14})RuCl\}_2(\mu\text{-paa})]^+$ when the arene ligand is *p*-cymene. The ligand paa is flexible around C1–C2 and N2–N3 single bonds (Fig. 5). Optimized structure [DFT/B3LYP/6-311G(d)] of the *trans* paa is more stable by 3.65 kcal/mol than the corresponding *cis* paa. The following questions are addressed in our work: (i) why paa forms mononuclear complexes when the arene group is $\eta^6\text{-}C_6H_6$ or $\eta^6\text{-}C_6Me_6$ and binuclear complex with $\eta^6\text{-}C_{10}H_{14}$; (ii) to what extent does the Ru–N bond distances and Ru–paa interaction energy alter when arene ligand changes from $\eta^6\text{-}C_6H_6$, $\eta^6\text{-}C_6Me_6$ to $\eta^6\text{-}C_{10}H_{14}$ and what are the relative strengths of Ru–C(η^6-arene) bonds and the flow of net electronic charge from η^6-arene to ruthenium; (iii) are there significant differences among deformation of coordinated paa ligand (rotation about N2–N3 and C1–C2 bonds) in **I**–**III**; (iv) how much does electronic charge flow from paa to metal fragment $[(\eta^6\text{-arene})RuCl]^+$?

In this paper, we report synthesis, spectral and electrochemical characterization of mono and binuclear complexes resulting from interaction of arene ruthenium complexes $[\{(\eta^6\text{-arene})RuCl(\mu\text{-}Cl)\}_2]$ with paa, pbp or bbp. We also present herein, molecular structures of the paa containing representative mononuclear complex $[(\eta^6\text{-}C_6Me_6)RuCl(paa)]BF_4$ (**1**), binuclear complex $[\{(\eta^6\text{-}C_{10}H_{14})RuCl\}_2(\mu\text{-paa})](BF_4)_2$ (**3**) and analogous pbp containing binuclear complex $[\{(\eta^6\text{-}C_{10}H_{14})RuCl\}_2(\mu\text{-pbp})](BF_4)_2$ (**6**), interaction studies (hydrogen bonding and π–π stacking) and DFT calculations on the complexes $[(\eta^6\text{-arene})RuCl(paa)]^+$.

2. Experimental

2.1. Materials

Analar grade chemicals were used throughout. All the synthetic manipulations were performed under oxygen

free dry nitrogen atmosphere. Solvents were dried and distilled before use following the standard literature procedures. Hydrated ruthenium(III)chloride, α-terpinene, hexamethylbenzene, pyridine-2-carbaldehyde, 1,4-phenylenediamine, benzidine, tetrabutylammonium perchlorate, ammonium hexafluorophosphate and ammonium tetrafluoroborate were obtained from Aldrich Chemical Company, Inc., USA and were used without further purification. The precursor complexes [{(η^6-arene)RuCl(μ-Cl)}$_2$] (arene = benzene, *p*-cymene or hexamethylbenzene) and the ligands pyridine-2-carbaldehyde azine (paa), *p*-phenylene-bis(picoline)-aldimine (pbp), *p*-biphenylene-bis(picoline)-aldimine (bbp) were prepared and purified by the literature procedures [3b,4b,7].

2.2. Instrumentation

Micro-analytical data on the complexes were obtained from Micro-analytical Laboratory of the Sophisticated Analytical Instrument Facility, Central Drug Research Institute Lucknow. IR spectra in Nujol mull in the region 4000–400 cm^{-1} and UV were recorded on a Shimadzu – 8201 PC and Shimadzu UV-1601 spectrophotometers, respectively. ^1H and ^{13}C NMR spectra with tetramethylsilane as the internal reference were obtained on a Bruker DRX-300 NMR machine at room temperature. MS spectra were recorded on a JEOL SX 102/DA-6000 Mass spectrometer system using Xenon as the FAB gas (6 kV and 10 mA). The accelerating voltage was 10 kV and spectra were recorded at room temperature using *m*-nitrobenzyl alcohol as the matrix. The CV were recorded on a Bio-analytical system CV-27 with C1B cell stand in de-aerated acetonitrile in presence of 0.2 M tetrabutylammonium perchlorate (TBAP) as supporting electrolyte, using three electrode assembly platinum working and counter electrodes and Ag/AgCl as reference electrode.

2.3. Preparation of complexes

2.3.1. [{(η^6-C_6Me_6)RuCl}(paa)]BF_4 (**1**)

A suspension of the complex [{(η^6-C_6Me_6)RuCl(μ-Cl)}$_2$] (0.668 g and 1.0 mmol) in methanol (30 mL) was treated with paa (0.420 g, 2.0 mmol) and allowed to stir at room temperature. The resulting solution was further stirred for ~4.0 h and filtered through celite to remove any solid impurities. To the filtrate, a saturated solution of NH_4BF_4 dissolved in methanol (10 mL) was added and left in refrigerator for slow crystallization. After a couple of days deep red colour microcrystalline compound separated. It was filtered washed with methanol, diethyl ether and dried in vacuo. The product was further recrystallized from dichloromethane/petroleum ether (40–60). (0.617 g and 87%). Anal. Calc. for $BC_{24}ClF_4H_{28}N_4Ru$: C, 48.32; H, 4.69; N, 9.39%, *M* 596. Found: C, 48.24; H, 4.41; N, 9.22%. *M* 596. λ_{max}/nm, dmso; (ε/$dm^3\,mol^{-1}\,cm^{-1}$) 427 (5,336), 299 (30,231), $_H$(300 MHz; $CDCl_3$; $SiMe_4$, *J* Hz): δ 9.73 (1H, d, 3.9); 8.45 (1H, t, 6.6); 8.08 (1H, t, 1.8); 9.27 (1H, d, 5.4); 8.81 (1H, s); 9.16 (1H, d, 3.1); 8.13 (1H, t, 5.7); 8.29 (1H, t, 2.5); 8.17 (1H, d, 5.4); 8.40 (1H s,); 2.07 (18H, s). $_C$(300 MHz; $CDCl_3$; $SiMe_4$): δ 156.1, 139.8, 131.3 and 130.0 (pyridyl carbons); 165.8 (N=*C*H); 90.1 $C_6(CH_3)_6$; 19.6 $C_6(CH_3)_6$. *m/z* 509 (M^+); 474 ($M^+ - Cl$); 311 ($M^+ - Cl–C_6Me_6$).

2.3.2. [{(η^6-C_6H_6)RuCl}$_2$(μ-paa)]$(BF_4)_2$ (**2**)

This complex was prepared by a suspension of the complex [{(η^6-C_6H_6)RuCl(μ-Cl)}$_2$] (0.500 g and 1.0 mmol) in methanol (30 mL) was treated with paa (0.210 g and 1.0 mmol) in 1:1 molar ratio. It separated as purple colour microcrystalline solid. It was filtered, washed with methanol, diethyl ether and dried in vacuo. The product was further recrystallized from dichloromethane/petroleum ether (40–60). (0.565 g and 67%). Anal. Calc. $B_2C_{24}Cl_2F_8\,H_{22}N_4Ru_2$: C, 35.42; H, 2.70; N, 6.88%. *M* 813. Found: C, 35.56; H, 2.51; N, 6.67%. *M* 813. λ_{max}/nm, dmso; (ε/$dm^3\,mol^{-1}\,cm^{-1}$) 421.50 (9,411), 317.5 (25,309), 260 (7,717). $_H$(300 MHz; $CDCl_3$; $SiMe_4$, *J* Hz): δ 9.42 (2H, d, 4.9); 7.45 (2H, t, 6.6); 7.38 (2H, t, 1.8); 8.27 (2H, d, 5.4); 8.12 (1H, s); 6.12 (6H, s); *m/z* 639 ($M^+ - 2BF_4$); 483 ($M^+ - 2C_6H_6$); 412 ($M^+ - 2Cl$).

2.3.3. [{(η^6-$C_{10}H_{14}$)RuCl}$_2$(μ-paa)]$(BF_4)_2$ (**3**)

This complex was prepared by following the abovementioned procedure (**2**) except that the complex [{(η^6-$C_{10}H_{14}$)RuCl(μ-Cl)}$_2$] was used in place of [{(η^6-C_6H_6)RuCl(μ-Cl)}$_2$]. It isolated as yellow-red *microcrystalline* solid. It was filtered, washed with methanol, diethyl ether and dried in vacuo. The product was further recrystallized from dichloromethane/petroleum ether (40–60°). (0.645 g and 82%). Anal. Calc. $B_2C_{32}Cl_2F_8H_{38}N_4Ru_2$: C, 41.51; H, 4.10; N, 6.05. *M* 926. Found: C, 41.37; H, 4.03; N, 6.01%. *M* 926. λ_{max}/nm, dmso; (ε/$dm^3\,mol^{-1}\,cm^{-1}$) 426.5 (9,933), 298 (25,981), $_H$(300 MHz; $CDCl_3$; $SiMe_4$, *J* Hz): δ 9.76 (2H, d, 5.4); 8.45 (2H, t, 7.2); 8.09 (2H, t, 7.8); 9.59 (2H, d, 7.5); 8.80 (2H, s); 6.33 (4H, AB); 2.95 (1H, sep, 3.8); 2.36 (3H, s); 2.04 (6H, d, 2.1). $_C$(300 MHz; $CDCl_3$; $SiMe_4$): δ 157.1, 140.8, 133.3, 131.0 (pyridyl carbons); 167.8 (N=*C*H); 106.4 (*C*–CH$(CH_3)_2$); 101.7 (*C*–CH_3); 4.7 (C_6H_4); 29.2 (*C*H$(CH_3)_2$); 22.4 (CH(*C*$H_3)_2$); 18.8 (C–*C*H_3). *m/z*; 752 ($M^+ - 2BF_4$); 484 ($M^+ - 2BF_4$–$2C_{10}H_{14}$); 413 ($M^+ - 2BF_4$–$2C_{10}H_{14}$–2Cl).

2.3.4. [{(η^6-C_6Me_6)RuCl}$_2$(μ-paa)]$(BF_4)_2$ (**4**)

This complex was prepared by following the abovementioned procedure (**2**) except that the complex [{(η^6-C_6Me_6)RuCl(μ-Cl)}$_2$] was used in place of [{(η^6-C_6H_6)RuCl(μ-Cl)}$_2$]. It separated in the form of

orange-red microcrystalline solid. (0.563 g and 64%). Anal. Calc. $B_2C_{36}Cl_2F_8H_{46}N_4Ru_2$: C, 44.03; H, 4.68; N, 5.70. *M* 981. Found: C, 44.21; H, 4.53; N, 5.45%. *M* 981. λ_{max}/nm, dmso; (ε/dm^3 mol^{-1} cm^{-1}) 427 (8,291), 301 (45,795), $_H$(300 MHz; $CDCl_3$; $SiMe_4$, *J* Hz): δ 9.84 (2H, d, 3.9); 8.56 (2H, t, 6.6); 8.12 (2H, t, 1.8); 9.31 (2H, d, 5.4); 8.33 (1H, s); 2.11 (18H, s); *m*/*z*; 807 ($M^+ - 2BF_4$); 483 ($M^+ - 2BF_4$–$2C_6Me_6$); 412 ($M^+ - 2BF_4$–$2C_6Me_6$–2Cl).

2.3.5. [{(η^6-C_6H_6)RuCl}$_2$(μ-pbp)](BF$_4$)$_2$ (**5**)

In a typical reaction a suspension of the complex [{(η^6-C_6H_6)RuCl(μ-Cl)}$_2$] (0.50 g and 1.0 mmol) in methanol (30 mL) was treated with pbp (0.286 g and 1 mmol) It isolated in the form of brown-black microcrystalline solid. (0.445 g and 68%). Anal. Calc. $B_2C_{30}CI_2F_8H_{26}N_4Ru_2$: C, 40.49; H, 2.92; N, 6.29. *M* 889. Found: C, 40.31; H, 2.72; N, 6.19%. *M* 889. λ_{max}/nm, dmso; (ε/dm^3 mol^{-1} cm^{-1}) 499 (4,321), 416 (7,894), 326 (11,444), 292 (12,885). $_H$(300 MHz; $CDCl_3$; $SiMe_4$, *J* Hz): δ 9.02 (2H, d, 5.7); 8.01 (2H, t, 5.2); 7.93 (2H, t, 5.4); 8.18 (2H, d, 4.8); 8.44 (2H, s); 6.22 (4H, m, 5.6); 6.13 (6H, s).

2.3.6. [{(η^6-$C_{10}H_{14}$)RuCl}$_2$(μ-pbp)](BF$_4$)$_2$ (**6**)

In a typical reaction a suspension of the complex [{(η^6-$C_{10}H_{14}$)RuCl(μ-Cl)}$_2$] (0.612 g and 1.0 mmol) in methanol (30 mL) was treated with pbp (0.286 g and 1 mmol). The dark-red crystalline substance thus obtained was filtered, washed with a little of methanol, diethyl ether and dried in vacuo. It was recrystallized from acetone/diethyl ether. (0.843 g and 89%). Anal. Calc. $B_2C_{38}Cl_2F_8H_{42}N_4Ru_2$: C, 45.55; H, 4.19; N, 5.59. *M* 1001. Found: C, 45.40; H, 4.11; N, 5.79%. *M* 1001. λ_{max}/nm, dmso; (ε/dm^3 mol^{-1} cm^{-1}) 422 (12,006), 337.5 (30,216), 295 (25,615), $_H$(300 MHz; $CDCl_3$; $SiMe_4$, *J* Hz): δ 9.06 (2H, d, 4.8); 8.35 (2H, t, 6.6); 7.97 (2H, t, 5.2); 8.47 (2H, d, 1.5); 8.17 (2H, s); 6.17 (4H, m, 5.2); 5.84 (4H, AB, 6.3); 2.84 (1H, sep, 5.7); 2.26 (3H, s); 2.00 (6H, d, 2.1). $_C$(300 MHz; $CDCl_3$; $SiMe_4$, *J* Hz) δ 157.0, 124.9, 140.9 (pyridyl carbons); 169.1, 130.2, 131.4 (N=*C*H and *p*-phenylene carbons); 107.5 (*C*–$CH(CH_3)_2$); 101.4 (*C*–CH_3); 85.6 (C_6H_4); 29.6 (*C*H$(CH_3)_2$); 21.3 (CH(*C*H$_3$)$_2$); 15.9 (C–*C*H$_3$). *m*/*z*; 827 ($M^+ - 2BF_4$); 559 ($M^+ - 2BF_4$–$2C_{10}H_{14}$); 488 ($M^+ - 2BF_4$–$2C_{10}H_{14}$–2Cl).

2.3.7. [{(η^6-C_6Me_6)RuCl}$_2$(μ-pbp)](BF$_4$)$_2$ (**7**)

This complex was prepared following the above procedure **5** except that the complex [{(η^6-C_6Me_6)RuCl(μ-Cl)}$_2$] was used in place of [{(η^6-C_6H_6)RuCl(μ-Cl)}$_2$]. It separated in the form of brown micro-crystalline solid. (0.714 g and 73%). Anal. Calc. $B_2C_{42}CI_2F_8H_{50}N_4Ru_2$: C, 47.68; H, 4.73; N, 5.29. *M* 1057. Found: C, 47.41; H, 4.43; N, 5.11%. *M* 1057. λ_{max}/nm, dmso; (ε/dm^3 mol^{-1} cm^{-1}) 435 (9,519), 319 (27,309), 294 (26,759) $_H$(300 MHz; $CDCl_3$; $SiMe_4$, *J* Hz): δ 9.20 (2H, d, 5.4); 8.13 (2H, t, 6.6); 7.90 (2H, t, 1.5); 8.32 (2H, d, 4.2); 8.19 (2H, s); 6.19 (4H, m, 5.7); 2.21 (18H, s). $_C$(300 MHz; $CDCl_3$; $SiMe_4$, *J* Hz): 155.0, 122.9, 138.9 (pyridyl carbons); 167.1, 129.2, 130.0 (N=*C*H and *p*-phenylene carbons); 93.5 $C_6(CH_3)_6$; 18.6 $C_6(CH_3)_6$.

2.3.8. [{(η^6-C_6H_6)RuCl}$_2$(μ-bbp)](BF$_4$)$_2$ (**8**)

In a typical reaction a suspension of the complex [{(η^6-C_6H_6)RuCl(μ-Cl)}$_2$] (0.50 g and 1.0 mmol) in MeOH (30 mL) was treated with bbp (0.362 g and 1.0 mmol) and resulting solution was heated under reflux for blue-green. After cooling at room temperature, it was filtered through celite to remove any solid residue. To the filtrate, a saturated solution of NH_4BF_4 dissolved in methanol (10 mL) was added and left in refrigerator for slow crystallization. After a couple of days deep red colour *microcrystalline* compound separated. It was filtered, washed with methanol, diethyl ether and dried in vacuo. The product was further recrystallized from dichloromethane/petroleum ether (40–60°). (0.872 g and 78%). Anal. Calc. $B_2C_{36}Cl_2F_8H_{30}N_4Ru_2$: C, 44.69; H, 3.10; N, 5.80. *M* 965. Found: C, 44.33; H, 3.04; N, 5.61.% *M* 965. λ_{max}/nm, dmso; (ε/dm^3 mol^{-1} cm^{-1}) 363.5 (38,528), 293 (39,402). $_H$(300 MHz; $CDCl_3$; $SiMe_4$, *J* Hz): δ 9.24 (2H, d, 4.8); 8.45 (2H, t, 6.6); 7.54 (2H, t, 5.2); 8.32 (2H, d, 1.5); 8.14 (2H, s); 6.67 (4H, dd); 6.17 (6H, sh.s., C_6H_6). $_C$(300 MHz; $CDCl_3$; $SiMe_4$, *J* Hz): δ 154.0, 122.0, 139.0 (pyridyl carbons); 169.9, 131.3–133.7 (N=*C*H and *p*-bisbisphenylene carbons); 93.2 (C_6H_6) *m*/*z*; 791 ($M^+ - 2BF_4$); 635 ($M^+ - 2BF_4$–$2C_6H_6$); 564 ($M^+ - 2BF_4$–$2C_6H_6$–2Cl).

2.3.9. [{(η^6-$C_{10}H_{14}$)RuCl}$_2$(μ-bbp)](BF$_4$)$_2$ (**9**)

It was prepared by above procedure **8** except that the complex [{(η^6-$C_{10}H_{14}$)RuCl(μ-Cl)}$_2$] was used in place of [{(η^6-C_6H_6)RuCl(μ-Cl)}$_2$]. It gives brown-red complex. (0.693 g and 87%). Anal. Calc. $B_2C_{44}Cl_2F_8H_{46}N_4Ru_2$: C, 49.02; H, 4.27; N, 5.19. *M* 1077. Found: C, 49.13; H, 4.12; N, 5.23%. *M* 1077. λ_{max}/nm, dmso; (ε/dm^3 mol^{-1} cm^{-1}) 364.5 (38,528), 292 (29,483). $_H$(300 MHz; $CDCl_3$; $SiMe_4$, *J* Hz): δ 9.03 (2H, d, 4.8); 8.23 (2H, t, 6.6); 7.67 (2H, t, 5.2); 8.32 (2H, d, 1.5); 8.13 (2H, s); 6.43 (4H, m); 5.45 (4H, AB, 6.3); 2.64 (1H, sep, 5.7); 2.23.(3H, s); 2.00 (6H, d, 2.1). $_C$(300 MHz; $CDCl_3$; $SiMe_4$, *J* Hz): 156.0, 123.0, 140.0 (pyridyl carbons); 168.7, 130.3, 133.4 (N=*C*H and *p*-bisphenylene carbons); 105.3 (*C*–$CH(CH_3)_2$); 102.6 (*C*–CH_3); 85.6 (C_6H_4); 29.4 (*C*H$(CH_3)_2$); 22.1 (CH(*C*H$_3$)$_2$); 18.8 (C–*C*H$_3$).

2.3.10. [{(η^6-C_6Me_6)RuCl}$_2$(μ-bbp)](BF$_4$)$_2$ (**10**)

It was prepared by above procedure **8** except that the complex [{(η^6-C_6Me_6)RuCl(μ-Cl)}$_2$] was used in place of [{(η^6-C_6H_6)RuCl(μ-Cl)}$_2$]. It was separated as red-brown microcrystalline compound. (0.672 g and 76%).

Anal. Calc. $B_2C_{48}Cl_2F_8H_{54}N_4Ru_2$: C, 50.83; H, 4.76; N, 4.94. *M* 1133. Found: C, 50.68; H, 4.43; N, 4.89%. *M* 1133. λ_{max}/nm, dmso; (ε/dm^3 mol^{-1} cm^{-1}) 440 (12,612), 354 (36,375), 293 (39,909). $_H$(300 MHz; $CDCl_3$; $SiMe_4$, *J* Hz): 9.14 (2H, d, 4.8); 8.65 (2H, t, 6.6); 7.64 (2H, t, 5.2); 8.31 (2H, d, 1.5); 8.12 (2H, s); 6.46 (4H, m); 2.21 (18H, s). $_C$(300 MHz; $CDCl_3$; $SiMe_4$, *J* Hz): 152.0, 123.0, 137.0 (pyridyl carbons); 167.9, 130.3–133.6 (N=*C*H and *p*-bisbiphenylene carbons); 92.2 $C_6(CH_3)_6$; 18.3 $C_6(CH_3)_6$.

2.4. Crystal structure determination

Cell dimensions and intensity data for complexes **1**, **3** and **6** were recorded on Enraf-Nonius CAD-4 four-Circle automatic diffractometer employing graphite monochromated Mo Kα radiation ($\lambda = 0.70930$ Å) at 293(2) K. Diffracted intensities were collected with $\omega - 2$ theta scanning technique (2 theta range 4.0–50.0°). All the pertinent data for complexes **1**, **3** and **6** were given in Table 2.

The structure was solved by direct methods (SHELX 97) and refined by full-matrix least squares calculations on F^2 (SHELX 97) [8]. All the non-hydrogen atoms were refined anisotropically. The hydrogen atoms were refined with isotropic thermal parameters fixed to those of the atoms to which they are bonded. The complexes **3** and **6** occupy special position, therefore only half of it are labelled. The computer programme PLATON was used for analyzing the interaction [8c].

CCDC reference numbers 183047, 183048 and 203553.

2.5. Theoretical calculations

Calculations were performed using the hybrid B3LYP density functional method, which uses Becke's 3-parameter nonlocal exchange functional [9] mixed with the exact (Hartree–Fock) exchange functional and Lee–Yang–Parr's nonlocal correlation functional [10]. The geometries of complexes [(η^6-arene)-RuCl(paa)]$^+$ (arene = C_6H_6, **I**; C_6Me_6, **II** and $C_{10}H_{14}$, **III**) were optimized without any symmetry restrictions with standard 6-31G(d) basis sets [11] for N, C, H elements and LANL2DZ [12] for Ru and Cl which combines quasi-relativistic effective core potentials with a valence double-basis set. Frequency calculations were performed to determine whether the optimized geometries were minima on the potential energy surface. The geometries of *trans*-paa and *cis*-paa were also optimized using 6-311G(d) basis sets. The electronic structures of the complexes were examined by NBO analysis [13] using 6-311G(d) basis sets for N, C, H elements and LANL2DZ for Ru and Cl elements. The calculations were carried out with the GAUSSIAN 98 program [14].

3. Results and discussion

Three different ligands imparting immine/azine hybrid-chelating N–N′ donor sites were chosen for the present study. The ligands paa, pbp or bbp have analogous coordination sites except that, in paa the azine nitrogen atoms are directly bonded with each other while those in pbp or bbp are separated by one or two phenyl spacers. These are expected to show interesting structural and electronic variations. The reactions of chloro-bridged arene ruthenium complexes [{(η^6-arene)RuCl(μ-Cl)}$_2$] with the bridging ligand paa, in the presence of an excess of the ligand or in equimolar ratio in methanol gives highly stable cationic mono and binuclear complexes [(η^6-arene)RuCl(paa)]$^+$ (arene = hexamethylbenzene) and [{(η^6-arene)RuCl}$_2$(μ-paa)]$^{+2}$ (arene = benzene, *p*-cymene or hexamethylbenzene) (Scheme 2).

Further, it was observed that, pbp or bbp under analogous reaction conditions upon reaction with [{(η^6-arene)RuCl(μ-Cl)}$_2$] in methanol, gave only binuclear complexes [{(η^6-arene)RuCl}$_2$(μ-L)]$^{+2}$ (Scheme 2). This observation is consistent with our earlier findings [6b]. The complexes have been isolated as their BF_4^- salts and purified by silica gel column. The yellow to blue brown cationic complexes resulting from these reactions are high melting, non-hygroscopic, air stable, shiny crystalline solids. These are sparingly soluble in methanol, benzene, soluble in acetone, dichloromethane, chloroform, acetonitrile, dimethysulfoxide, dimethylformamide, and insoluble in petroleum ether and diethyl ether.

Analytical data of the complexes conformed well to their respective formulations. Further information about composition of the complexes has also been obtained from MS spectroscopy. Spectral data of the complexes are recorded in Section 2. The position of different peaks and overall fragmentation patterns are in excellent agreement with the formulation of the complexes and strongly support mono and binuclear nature of the complexes.

Infrared spectra of the complexes exhibit characteristic band due to pyridyl ring vibrations of the ligands along with the characteristic bands corresponding to counter anions. The ν_{C-N} band in the complexes shifted towards lower wave numbers and appeared around 1612 cm^{-1}, as compared to that in free ligand (1638 cm^{-1}). The bands associated with pyridyl ring breathing mode appeared at about 1032 cm^{-1}. The shift in the position of ν_{C-N} and breathing mode suggested that co-ordination of the metal ion through pyridyl and diazine nitrogen [3b]. Broad bands in the region 1118 cm^{-1} have been assigned to counter anion BF_4^-.

^{1}H and ^{13}C NMR spectral data of the complexes are summarized in Section 2 and these are in good agreement with the proposed molecular formula. ^{1}H NMR spectra of the mononuclear complex **1** [{(η^6-

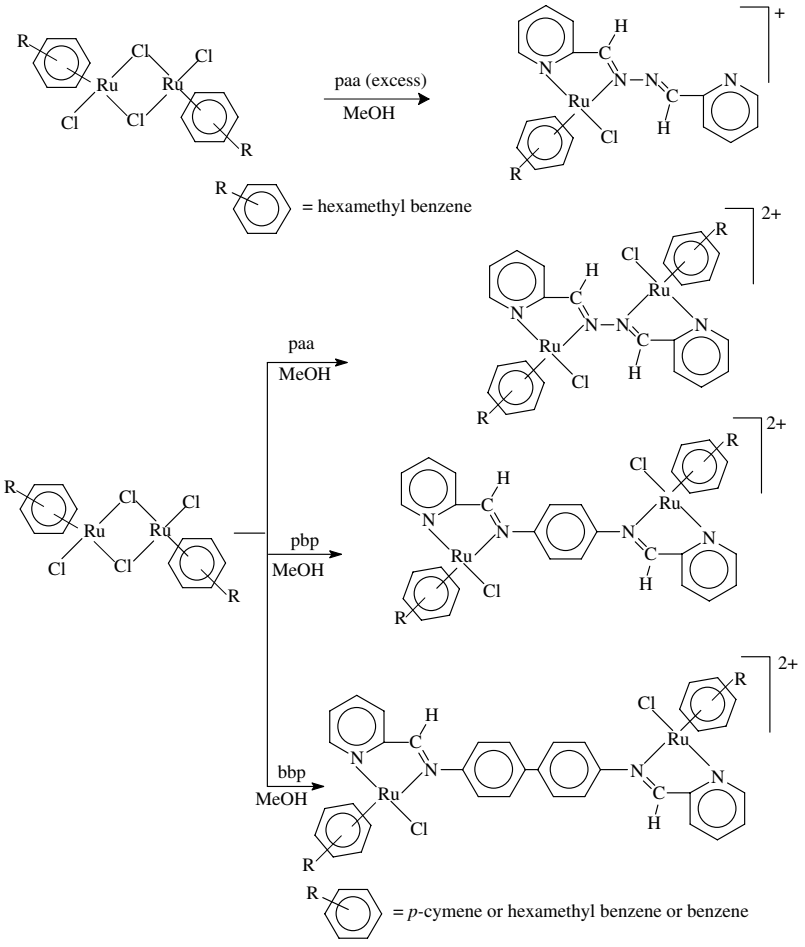

Scheme 2.

C_6Me_6)RuCl}(paa)]$^+$ exhibited 10 distinct resonances (recorded in Section 2) assignable to pyridyl ring and N=CH protons of the ligand paa. These protons exhibited down field shift as compared to that in free ligand, upon coordination with the metal center [3a,15]. The hexamethylbenzene ring protons resonated as a singlet at δ 2.07 (18H, s). $^{13}C\{^1H\}$ NMR spectra of the complex **1** followed the trends observed in the ^1H NMR spectra. The paa carbons in complex **1** resonated at δ 156.1; 139.8; 131.3; 130.0 ppm (pyridyl carbons), 165.8 ppm (N=*C*H), where as hexamethylbenzene carbons resonated at δ 90.1 ppm ($C_6(CH_3)_6$) and 19.6 ppm ($C_6(CH_3)_6$) [5b].

The ^1H NMR spectra of the binuclear complexes **2**–**4** [{(η^6-arene)RuCl}$_2$(μ-L)]$^{+2}$ (arene = benzene, *p*-cymene or hexamethylbenzene; L = paa) displayed only five distinct resonances two doublets at δ 9.76 and δ 9.59, two triplets at δ 8.45 and δ 8.09 and one singlets at δ 8.80 ppm, respectively, assignable to paa protons. The arene protons (benzene, *p*-cymene, hexamethylbenzene) in the complexes resonated at δ 6.12 (6H, s); δ 6.33 (4H, AB, 6.0); 2.95 (1H, sep, 3.7); 2.36 (3H, s); 2.04 (6H, d, 2.1) ppm and δ 2.11 ppm, respectively, which indicated that two [(η^6-arene)RuCl] moieties are bridged by paa in highly symmetrical manner. It accounts well for a single, highly symmetrical species, in which, two arene rings are *trans* disposed with respect to the paa ligand. This has further been supported by single crystal X-ray diffraction studies and DFT calculations (vide infra). The ^1H NMR spectra of the pbp and bbp complexes **5**–**10** followed the general trends as observed in the ^1H NMR spectra of complexes **2**, **3** or **4**. Along-with the pyridyl and arene protons, it also exhibited additional resonances in the region δ 6.17 (m), 6.67 (m) ppm, corresponding to aromatic protons of the phenyl group of pbp and bbp. The position and integrated intensity of different signals corroborated well to the formulation of the complexes. The presence of different signals suggested that pbp or bbp forms a symmetrical bridge between the ruthenium centers in which, two [(η^6-arene)RuCl] moieties are *trans* disposed with respect to the ligand. This observation is consistent with our earlier report [6b].

The complexes may exist as diastereomers, but all efforts to separate the diastereomers were unsuccessful at our hands. However, it has been supported by ill-resolved NMR data. In the respective spectra, signals for the minor diastereomer is hidden or not well resolved,

Table 1
Electrochemical data of the complexes

Serial no.	Complex	Oxidation first		Reduction first	
		E_{pa} (V)	E_{pc} (V)	E_{pa} (V)	E_{pc} (V)
1	$[\{(\eta^6\text{-}C_6Me_6)RuCl\}(paa)](BF_4)$ (**1**)	1.7	−0.25, −0.80, −1.60	1.1, 1.7	−0.8, −1.60
2	$[\{(\eta^6\text{-}C_6H_6)RuCl\}_2(\mu\text{-}paa)](BF_4)_2$ (**2**)	–	−0.34, −1.1	1.1	−0.30, −1.15
3	$[\{(\eta^6\text{-}C_{10}H_{14})RuCl\}_2(\mu\text{-}paa)](BF_4)_2$ (**3**)	–	−0.34, −1.1	1.1, 1.4	−0.31, −1.1
4	$[\{(\eta^6\text{-}C_6Me_6)RuCl\}_2(\mu\text{-}paa)](BF_4)_2$ (**4**)	1.70	−0.2, −0.80, −1.1	1.1	−0.8, −1.1
5	$[\{(\eta^6\text{-}C_6H_6)RuCl\}_2(\mu\text{-}pbp)](BF_4)_2$ (**5**)	1.1	−0.4, −1.1, −1.4	1.1	−0.7, −1.1, −1.4
6	$[\{(\eta^6\text{-}C_{10}H_{14})RuCl\}_2(\mu\text{-}pbp)](BF_4)_2$ (**6**)	1.7	−0.2, −0.7, −1.1	1.1	−0.7, −1.1
7	$[\{(\eta^6\text{-}C_6Me_6)RuCl\}_2(\mu\text{-}pbp)](BF_4)_2$ (**7**)	1.5	−1.0	1.1	−1.1, 1.7
8	$[\{(\eta^6\text{-}C_6H_6)RuCl\}_2(\mu\text{-}bbp)](BF_4)_2$ (**8**)	1.0, 1.8	−0.3, −0.7, −1.1	1.1	−0.7, −1.3
9	$[\{(\eta^6\text{-}C_{10}H_{14})RuCl\}_2(\mu\text{-}bbp)](BF_4)_2$ (**9**)	1.7	−0.7, −1.1, −1.6	1.1	−0.7, −1.1, −1.6
10*	$[\{(\eta^6\text{-}C_6Me_6)RuCl\}_2(\mu\text{-}bbp)](BF_4)_2$ (**10**)	1.5	−0.3, −1.1	1.1	−1.1

* $E_{1/2} = 1.3$ V.

therefore, we are unable to make precise interpretation of the different signals. In the present manuscript, we have taken into account major isomer.

The low spin d^6 configuration of both the mono and binuclear complexes resulting from interaction of the chloro-bridged arene ruthenium complexes $[\{(\eta^6\text{-arene})RuCl(\mu\text{-}Cl)\}_2]$ (arene = benzene, *p*-cymene or hexamethylbenzene) with the bridging ligands paa, pbp or bbp provide filled orbitals of proper symmetry on Ru(II), which, interact with the low lying π^* orbitals of the ligand. One should, therefore, expect a band attributable to MLCT transition $Ru(d\pi \rightarrow \pi^*)$ in the complexes. Furthermore, the energy of these transitions should vary with the nature of the ligands.

Electronic spectra of the mononuclear complex **1** displayed bands at 427 and 299 nm in acetonitrile. The band at 427 nm has been assigned to MLCT transition arising due to transfer of charge density from the filled $d\pi$ orbitals of Ru(II) to low lying π^* orbitals of the N-donor polypyridyl ligand, i.e, $[Ru(d\pi) \rightarrow \pi^*(paa)]$ bands. The band centered at 299 nm has been assigned to metal-perturbed LC transition. Three distinct peaks were observable in the region 499–420, 365–320 and at about 290 nm. The low energy bands present in the visible region at ~499–420 nm has been assigned to metal-to-ligand charge transfer (MLCT) transitions $[Ru(d\pi) \rightarrow \pi^*(L)]$ (L = paa, pbp or bbp). Absorption bands below 400 nm composed of second MLCT, ligand field or intra-ligand transitions ($\pi \rightarrow \pi^*$).

Ambiguous behaviour of arene complexes (mono and binuclear) also depends upon the sterically bulky arene precursor complexes. $[RuCl(\eta^6\text{-}C_6Me_6)]^+$ is sterically bulkier than its benzene or *p*-cymene counterparts, coordination to the uncoordinated paa function of $[RuCl(\eta^6\text{-}C_6Me_6)(paa)]^+$ is hindered. The steric effect attenuates if there are spacer groups between the imine units, as in pbp and bbp, thus accounting for the exclusive formation of the binuclear dications in these cases [6b].

The CV were recorded in acetonitrile using a single compartment electrochemical cell utilizing platinum working and counter electrodes and Ag/AgCl as reference electrode with the 0.2 M tetrabutylammonium perchlorate (TBAP) as supporting electrolyte. The results are summarized in Table 1 and representative scan of the complex $[\{(\eta^6\text{-}C_6Me_6)RuCl\}_2(\mu\text{-bbp})](BF_4)_2$ is given in Fig. 1.

The plots of peak current vs square root of the scan rate are linear indicating that diffusion-limiting process occur at the electrodes. The CV of the free ligand paa and pbp exhibit two reduction process at E_p, −1.49, −1.98 V and E_p, −1.57 V and E_2, −2.04 V, respectively, vs Ag/AgCl in acetonitrile [3b,16]. The CV scan of mononuclear complex **1** $[\{(\eta^6\text{-}C_6Me_6)RuCl\}(paa)]^+$ exhibits a irreversible metal-based oxidation M(**II**)/M(**III**) at E_{pa} 1.7 V and ligand-based reduction at E_{pc} −0.25, −0.80, −1.60 V in acetonitrile at scan rate 200 mV/s. In binuclear complexes, additional oxidative and reductive waves are observed, as compared with mononuclear complex. The complex **10** exhibits metal-based oxidation at

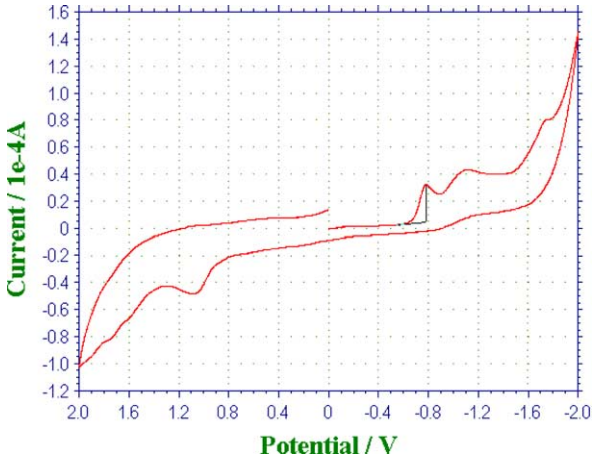

Fig. 1. Cyclic voltammogram for complex $[\{(\eta^6\text{-}C_6Me_6)RuCl\}_2(\mu\text{-bbp})](BF_4)_2$.

E_{pa} 1.50 V and ligand-based reduction at E_{pc} −0.3 and −1.1 V ($E_{1/2}$ at 1.3 V). In binuclear complexes, two closely spaced metal-centered oxidation waves are observed, possibly due to successive oxidation of the individual metal centers. In these complexes, the oxidation waves are observed at significantly more positive potentials compared to that in mononuclear complexes. Summarily the reduction waves also show anodic shift vis-a-vis mononuclear complexes [17]. Upon coordination to metal, in the complexes the ligand reduction potential shifts by 0.60–0.80 V to the positive side. Since, the pbp and bbp free ligands do not exhibit an oxidative peaks between 0 and +2.0 V vs Ag/AgCl, therefore, the oxidation waves in this region in the complexes **5**–**10**, seems to arise due to Ru(II)/Ru(III) process.

All ligand-centered reductions in complexes are easier than that in the free ligands. In case of binuclear complexes this decreases in the order of L = paa > pbp > bbp, which may be due to increase in competitive interaction with diimine moieties, partially due to extent of π conjugation in the ligands. The paa ligand having higher degree of π conjugation, closely binds with two [(η^6-arene)RuCl] moieties. The Ru–N distance in paa complex is shorter than that in the pbp and bbp suggesting greater σ, π interactions [3b]. This observation is consistent with the results obtained from single crystal X-ray diffraction and DFT studies (vide supra).

Molecular structures of the representative pyridine-2-carbaldehyde azine (paa) containing mono and binuclear complexes [(η^6-C_6Me_6)RuCl(paa)]BF_4 (**1**) and [{(η^6-$C_{10}H_{14}$)RuCl}$_2$(μ-paa)]$(BF_4)_2$ (**3**) and *p*-phenylenebis-(picoline)-aldimine (pbp) containing complex [{(η^6-$C_{10}H_{14}$)RuCl}$_2$(μ-pbp)]$(BF_4)_2$ (**6**) have been determined by single crystal X-ray diffraction studies. The molecular structures of the complex cations are shown in Figs. 2–4 with details about data collection, structure solution and refinement in Table 2 and selected bond length, bond angles and torsion angles in Table 3.

The crystal packing in the complexes **1**, **3** and **6** is stabilized by C–H···X type (X = Cl, F) inter and intramolecular hydrogen bonding. Contact distances between C–H···F and C–H···Cl are 2.34–2.52 Å and 2.71–2.83 Å, respectively (Figures available in supplementary material). The packing in the complex **3** also shows π–π stacking interactions between pyridyl rings. The interplaner and the centroid-to-centroid distances between the pyridyl rings are 3.39 and 3.81 Å respectively for complex **3** [18e]. Relevant bond distances, bond angles and symmetry are summarized in Table 4, which agree well with standard reported values [18].

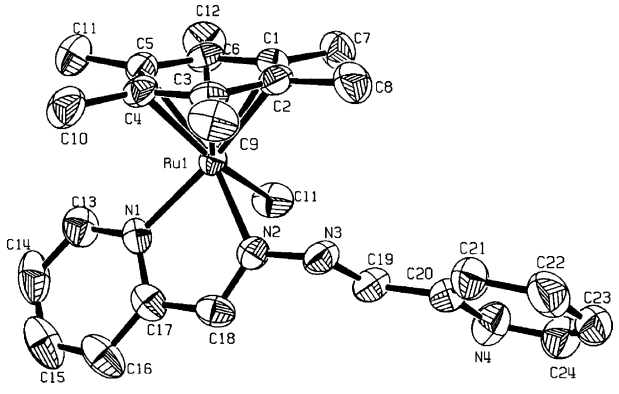

Fig. 2. Structure of the complex cation of **1**.

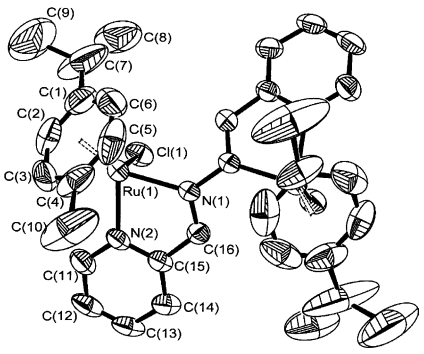

Fig. 3. Structure of the complex cation of **3**.

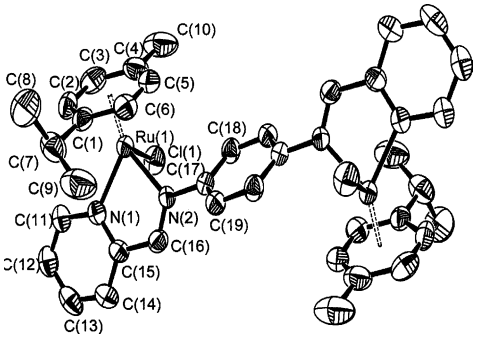

Fig. 4. Structure of the complex cation of **6**.

The immediate coordination sphere of the metal center ruthenium in all the three complexes **1**, **3** and **6** are essentially similar. Coordination sphere about the metal center ruthenium consists of the chloride group, pyridyl and azine nitrogen atoms from the paa or pbp ligand and arene ring; (η^6-C_6Me_6) in complex **1**, and (η^6-$C_{10}H_{14}$) ring in complexes **3** and **6**. Considering the arene ring as a single coordination site bonded in η^6 manner through the centroid, local coordination geometry about the metal center ruthenium in these complexes might be described as typical "piano-stool" geometry. The Ru–η^6–arene distances are comparable and are consistent with those reported in other Ru(II) complexes [5,19]. The inter-ruthenium distances in the binuclear complexes **3** and **6** are 5.137 and 8.487 Å, respectively, indicating the absence of a metal–metal bond. The Ru–Cl bond lengths are very similar in all the three complexes and are comparable to the average

Table 2
Crystal data and structure refinement parameters for complexes **1**, **3** and **6**

Name	Complex **1**	Complex **3**	Complex **6**
Empirical formula	$C_{24}H_{28}BClF_4N_4Ru$	$C_{16}H_{19}BClF_4N_2Ru$	$C_{38}H_{42}B_2Cl_2F_8N_4Ru_2$
Molecular weight	595.83	462.66	1001.42
Colour and habit	Orange red, Block	Yellow brown, Block	Shiny red, Plate
Crystal size (mm)	$0.22 \times 0.22 \times 0.17$	$0.4 \times 0.35 \times 0.35$	$0.4 \times 0.3 \times 0.3$
Space group	*Cc*	*Pcan*	$P2_1/n$
System	Monoclinic	Orthorhombic	Monoclinic
Unit cell dimensions			
a (Å)	17.0090(11)	12.801(3)	15.6690(19)
b (Å)	13.0030(7)	15.454(2)	17.2250(18)
c (Å)	12.1590(15)	18.971(4)	16.8210(14)
β (Å)	109.663(7)	90.000(17)	115.526(9)
V (Å^3)	2532.4(4)	3753.0(12)	4096.8(7)
Z	4	8	4
d_{calc} (g/cm^3)	1.563	1.638	1.624
μ (mm^{-1})	0.774	1.016	0.938
Temperature (K)	293 (2)	293 (2)	293 (2)
Number of reflections	2284	3026	6794
Number of refined para.	330	229	512
R factor all	0.0272	0.0564	0.0640
R factor [$I > 2\sigma(I)$]	0.0247	0.0501	0.0451
wR_2	0.0660	0.1520	0.1265
wR_2 [$I > 2\sigma(I)$]	0.0636	0.1582	0.1186
Goodness-of-fit	1.128	1.127	0.937

Table 3
Selected bond lengths (Å) bond angles (°) and torsion angles (°) for the complexes **1**, **3** and **6**

$[(\eta^6\text{-}C_6Me_6)RuCl(paa)]^+$		$[\{(\eta^6\text{-}C_{10}H_{14})RuCl\}_2(\mu\text{-paa})]^{+2}$		$[\{(\eta^6\text{-}C_{10}H_{14})RuCl\}_2(\mu\text{-pbp})]^{+2}$	
Ru(1)–N(1)	2.105(4)	Ru(1)–N(1)	2.108(4)	Ru(1)–N(1)	2.099(4)
Ru(1)–N(2)	2.072(4)	Ru(1)–N(2)	2.089(4)	Ru(1)–N(2)	2.055(4)
Ru(1)–C_{av}	2.218	Ru(1)–C_{av}	2.187	Ru(1)–C_{av}	2.2073
Ru(1)–Cl	2.3866(14)	Ru(1)–Cl(1)	2.3937(16)	Ru(1)–Cl(1)	2.3866(14)
Ru(1)–Ct	1.699	Ru(1)–Ct	1.694	Ru(2)–N(3)	2.076(4)
				Ru(2)–N(4)	2.092(4)
				Ru(2)–Cl(2)	2.3924(13)
				Ru(2)–C_{av}	2.198
				Ru(1)–Ct	1.702
				Ru(2)–Ct	1.688
N(1)–Ru(1)–N(2)	75.5(2)	N(1)–Ru(1)–N(2)	76.16(17)	N(2)–Ru(1)–N(1)	76.51(14)
N(1)–Ru(1)–Cl(1)	87.53(13)	N(1)–Ru(1)–Cl(1)	84. 41(12)	N(2)–Ru(1)–Cl(1)	85.57(11)
N(2)–Ru(1)–Cl(1)	83.89(13)	N(2)–Ru(1)–Cl(1)	85.47(13)	N(1)–Ru(1)–Cl(1)	83.35(11)
N(3)–N(2)–Ru(1)	123.4(3)	Ru(1)–N(1)–C(16)	117.1(3)	N(3)–Ru(2)–N(4)	75.91(15)
		Ru(1)–N(2)–C(15)	116.0(3)	N(3)–Ru(2)–Cl(2)	85.48(11)
		N(1)–N(1)–Ru(1)	127.9(4)	N(4)–Ru(2)–Cl(2)	86.28(11)
N(1)–Ru(1)–N(2)–N(3)	−178.3(5)	N(1)–Ru(1)–N(2)–C(11)	−176.3(5)	N(1)–Ru(1)–N(2)–C(17)	−174.2(4)
N(3)–C(19)–C(20)–N(4)	179.6(6)	N(1)*–N(1)–C(16)–C(15)	−175.0(4)	N(2)–Ru(1)–N(1)–C(11)	−177.1(4)
N(1)–C(17)–C(18)–N(2)	1.1(7)	N(1)–C(16)–C(15)–N(2)	−0.2(7)	N(4)–Ru(2)–N(3)–C(28)	174.9(4)
		Ru(1)–N(2)–C(15)–C(14)	−178.0(5)	C(17)–N(2)–C(16)–C(15)	176.8(4)
				N(1)–C(15)–C(16)–N(2)	−4.2(6)
				C(22)–N(4)–C(23)–C(24)	175.3(4)
				N(4)–C(23)–C(24)–N(3)	1.1(7)

bond length of 2.429 Å in the other Ru(II) complexes [20].

The Ru–N_{py} and Ru–N_{azine} bond distances and N–Ru–N bond angles are comparable in these complexes. In the mononuclear complex **1**, Ru–N_{azine} distance Ru–N(2) is 2.072(4) Å which is slightly shorter than Ru–N_{py} distance Ru–N(1) which is 2.105(4) Å. Analogous pattern is observed in the binuclear complex **3**, but in complex **6** the Ru–N_{azine} distances are shorter than Ru–N_{py} distances. The distances fall in the same range as observed in other pyridyl azo complexes [21].

In the complex **1**, the N(1)–Ru(1)–N(2) angle of 75.5(2)°, suggested inward bending of the coordinated pyridyl and azine group. At the same time, coordinated

Table 4
Hydrogen bonds in complex **1**, **3** and **6**

D–H···A	*d*(D–H)	*d*(H···A)	*d*(D···A)	∠(DHA)
*Complex **1** (Å and °)*[a]				
C(9)–H(9C)···Cl(1)#2	0.96	2.79	3.606(7)	143.8
C(10)–H(10C)···Cl(1)#2	0.96	2.72	3.658(7)	164.3
C(16)–H(16)···F(1)#1	1.15(14)	2.34(14)	3.38(2)	150(10)
*Complex **3** (Å and °)*[b]				
C(2)–H(2)···F(2)#3	0.93	2.38	3.294(13)	167.1
C(6)–H(6)···F(1)#2	0.93	2.44	3.189(14)	138.0
C(7)–H(7)···Cl(1)	0.98	2.83	3.449(13)	121.7
C(10)–H(10A)···F(1)#1	0.96	2.37	3.281(14)	158.1
C(11)–H(11)···F(4)#3	0.93	2.47	3.368(11)	162.9
C(13)–H(13)···Cl(1)#4	0.93	2.79	3.525(6)	136.9
C(14)–H(14)···F(3)#5	0.93	2.47	3.248(11)	140.7
*Complex **6** (Å and °)*[c]				
C(3)–H(3)···F(3)#3	0.93	2.47	3.226(8)	137.8
C(6)–H(6)···Cl(2)#4	0.93	2.71	3.460(5)	138.4
C(10)–H(10B)···F(1)#3	0.96	2.57	3.272(9)	129.9
C(16)–H(16)···F(4)#5	0.93	2.49	3.284(8)	143.7
C(20)–H(20)···F(6)#6	0.93	2.42	3.174(9)	138.5
C(23)–H(23)···F(8)#6	0.93	2.52	3.447(12)	176.7

[a] #1, x, y, z and #2, $x, -y+2, z+1/2$.
[b] #1, $x, -y, -z+1/2$; #2, x, y, z; #3, $-x+1/2, -y+1/2, z+1/2$; #4, $-x, -y, -z+1$ and #5, $x-1/2, y-1/2, -z+1/2$.
[c] #1, $-x, -y, -z$; #2, $-x+2, -y, -z+1$; #3, x, y, z; #4 $x-1, y, z$ and #5, $-x+1/2, y+1/2, -z+1/2$ and #6, $x+1/2, -y+1/2, z+1/2$.

part of the paa ligand is planar and the torsion angle C(18)–N(2)–N(3)–C(19) is 78.3(7)°. The torsion angles N(1)*–N(1)–C(16)–C(15) and N(2)–C(15)–C(16)–N(1) are −175.0(4)° and −0.2(7)° in the complex **3**, suggested that the ligand paa is not planar and the two [{(η^6-$C_{10}H_{14}$)RuCl}] units in the complex are closer to *trans* than *cis* configuration. It has further been confirmed by theoretical studies on the complexes [(η^6-arene)RuCl(paa)]$^+$. Similarly, in the complex **6** torsion angle N(1)–C(15)–C(16)–N(2) is −4.2(6)° and C(17)–N(2)–C(16)–C(15) is 176.8(4)°, suggesting that coordinated pyridyl and azine nitrogen atoms are lying almost in the same plane. At the same time, the torsion angles N(4)–C(23)–C(24)–N(3) and C(22)–N(4)–C(23)–C(24) are 1.1(7)° and 175.3(4)°, respectively, and indicated that, upon coordination with the ligand both the [(η^6-$C_{10}H_{14}$)RuCl] units in the complex assume *trans* rather than *cis* configuration.

The N(2)–N(3) distance in the complex **1** is 1.406(7) Å, which is comparable with that in hydrazine N–N single bond distance 1.47 Å. The C=N bond lengths are N(2)–C(18) and N(3)–C(19) are 1.281(7) and 1.273(8) Å, respectively, which are comparable and can be consider to have double bond character. The N(1)–N(1)* bond length of 1.414(8) Å in complex **3**, comparable with N–N bond length in hydrazine (1.47 Å) and that in complex **1** and can be defined as a N–N single bond [3g]. The C=N bond length N(1)–C(16) is 1.281(7) Å which is very close to C=N bond length in related uncoordinated ligands. The C=N bond lengths C(16)–N(2) and C(23)–N(4) in the complex **6** are 1.280(6) and 1.266(6) Å, respectively, and are comparable with those observed in the complexes **1** and **3**.

3.1. Theoretical study of the complexes [(η^6-arene)RuCl(paa)]$^+$

Fig. 5 shows the optimized geometry of the complexes [(η^6-arene)RuCl(paa)]$^+$ (arene = C_6H_6, **I**; C_6Me_6, **II**; $C_{10}H_{14}$, **III**), *trans* and *cis*-paa. The optimized bond lengths and angles at B3LYP are presented in Table 5. Both the *trans* and *cis*-paa are planar. The *cis*-paa is obtained from *trans*-paa by a rotation of 180° (about C1–C2 bond) and *trans*-paa is 3.65 kcal/mol more stable than the corresponding *cis*-paa. Coordinated paa ligand in the complexes **I**–**III** is non-planar. Two major distortions, rotation about N2–N3 and C1–C2 bonds, have been observed in coordinated paa ligand and are dependent on the arene ligand. The *p*-cymene complex **III** has an average Ru–C(arene) bond distance 2.289 Å which is the shortest Ru–C(arene) bond distance of the complexes investigated in this study. Similar results have been found by X-ray diffraction studies Table 5. The Ru–N1 and Ru–N2 bond distances are in the same order **II** > **I** > **III** as average Ru–C bond distances. We find greater deformation (variations in C1–N3–N2–C7 and N3–C1–C2–N4 in dihedral angles) of coordinated paa ligand in complex **III** from the equilibrium structure *trans*-paa Fig. 5 and Table 5. Smaller rotation about C1–C2 bond in **II** favours the formation of mononuclear complexes and these observations agree well with the experimental

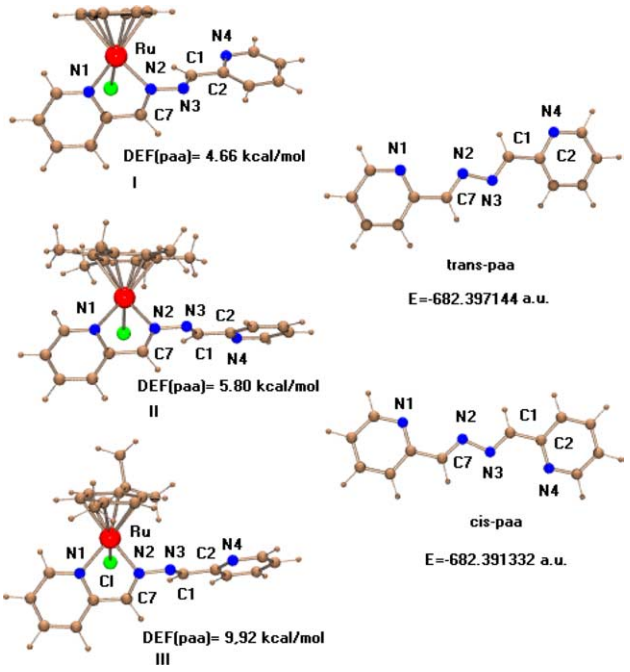

Fig. 5. Optimized geometries of the $[(\eta^6\text{-arene})RuCl(paa)]^+$ (arene = C_6H_6, **I**; C_6Me_6, **II**; $C_{10}H_{14}$, **III**).

results that the mononuclear complexes of paa with fragment $[(\eta^6\text{-}C_6Me_6)RuCl]^+$ have been isolated. On the other hand, the greater rotation about N2–N3 as well as C1–C2 bonds in paa upon interaction with fragment $[(\eta^6\text{-}C_{10}H_{14})RuCl]^+$ favours the formation of a binuclear complex. We begin the analysis of the bonding situation in the $[(\eta^6\text{-arene})RuCl(paa)]^+$ (arene = C_6H_6, **I**; C_6Me_6, **II**; $C_{10}H_{14}$, **III**) with a discussion of the conventional indices which are frequently used in order to characterize the bonding situation in molecules, i.e., bond orders and atomic charges. Table 6 gives the Wiberg bond indices (WBI) [22]. To examine the charge flow between the paa ligand and the $[(\eta^6\text{-arene})RuCl]^+$ metal fragments in the complexes **I**–**III**, we calculated the atomic charges of the fragment in the frozen geometries of the molecules. The results are shown in Figs. 6(a) and (b). Table 6 shows that the WBI values of the Ru–N bonds of the complexes **I**–**III** are in the range 0.44–0.47. It appears that in these complexes the Ru–N bonds would be significantly more polar with a bond order less than one.

The calculated charge distribution indicates that the ruthenium atom, arene and paa groups carry a significant positive charge while the chloro ligand is negatively charged. The charge on ruthenium is almost same (~+0.42) in these three complexes. Arene (C_6H_6, +0.70; C_6Me_6, +0.58; $C_{10}H_{14}$, +0.49) and paa (+0.31 in **I**, +0.49 in **II**, +0.56 in **III**) ligands in complexes **I**–**III**, shows interesting charge distributions. More interesting information is revealed when the charge flows between the interacting fragments paa and $[(\eta^6\text{-arene})RuCl]^+$ are compared. Fig. 6 shows, that the arene groups in complexes **II** and **III** have a lower positive charge than those in the respective metal fragments. We ascribe the flow of charge from paa ligand to $[(\eta^6\text{-arene})RuCl]^+$ to the polarization of paa in these complexes under the electrostatic field of the positively charged ruthenium atom

Table 5
Selected optimized geometrical parameters for the complexes $[(\eta^6\text{-arene})RuCl\ (paa)]^+$ (arene = C_6H_6, **I**; C_6Me_6, **II**; *p*-cymene, **III**)

	B3LYP	B3LYP	B3LYP	*trans*-paa
	I	**II**	**III**	
Bond distances				
Ru–N1	2.099	2.116	2.107	
Ru–N2	2.095	2.094	2.079	
Ru–Cl	2.451	2.476	2.471	
Ru–C(arene)$_{av.}$[a]	2.301	2.308	2.289	
N2–N3	1.383	1.386	1.376	1.414
N3–C1	1.289	1.288	1.287	1.281
C1–C2	1.463	1.468	1.469	1.456
Bond angles				
N1–Ru–N2	76.97	76.25	76.46	
N1–Ru–Cl	84.30	83.60	84.28	
N2–Ru–Cl	84.98	85.18	84.48	
N2–N3–C1	115.61	115.61	116.07	114.85
N3–C1–C2	122.06	121.67	121.71	116.72
C1–C2–N4	113.44	113.62	118.12	114.02
Dihedral angles				
C1–N3–N2–C7	146.01	105.92	98.84	140.8
N4–C2–C1–N3	−171.68	−173.49	−2.46	−0.3
N2–N3–C1–C2	−178.73	−179.87	177.86	−175.00

[a] av = average.

Table 6
Bonding energy (B.E.) and Wiberg bond indices (WBI) of the complexes $[(\eta^6\text{-arene})RuCl(paa)]^+$ (arene = C_6H_6, **I**; C_6Me_6, **II**; *p*-cymene, **III**)

	B.E. (kcal/mol)	WBI						
		Ru–N1	Ru–N2	Ru–Cl	Ru–C(arene)[a]	N2–N3	N3–C1	C1–C2
$[(\eta^6\text{-}C_6H_6)RuCl(paa)]^+$	−91.75	0.46	0.47	0.57	0.26	1.10	1.72	1.09
$[(\eta^6\text{-}C_6Me_6)RuCl(paa)]^+$	−79.45	0.44	0.46	0.51	0.25	1.07	1.76	1.08
$[(\eta^6\text{-}p\text{-cymene})RuCl(paa)]^+$	−84.31	0.44	0.45	0.53	0.27	1.09	1.76	1.08
$[(\eta^6\text{-}C_6H_6)RuCl]^+$	–	–	–	0.80	0.34	–	–	–
$[(\eta^6\text{-}C_6Me_6)RuCl]^+$	–	–	–	0.67	0.34	–	–	–
$[(\eta^6\text{-}p\text{-cymene})RuCl]^+$	–	–	–	0.74	0.35	–	–	–
trans-paa	–	–	–	–	–	1.11	1.74	1.08

[a] a = average.

in $[(\eta^6\text{-arene})RuCl]^+$. The change in charges of arene and Cl ligands provides the estimate of polarization effect. Sum of charges on arene and paa ligands is approximately +1.0. We note a direct relationship between net positive charge on coordinated paa ligand and its deformation (variations in C1–N3–N2–C7 and N3–C1–C2–N4 in dihedral angles) from the equilibrium structure *trans*-paa.

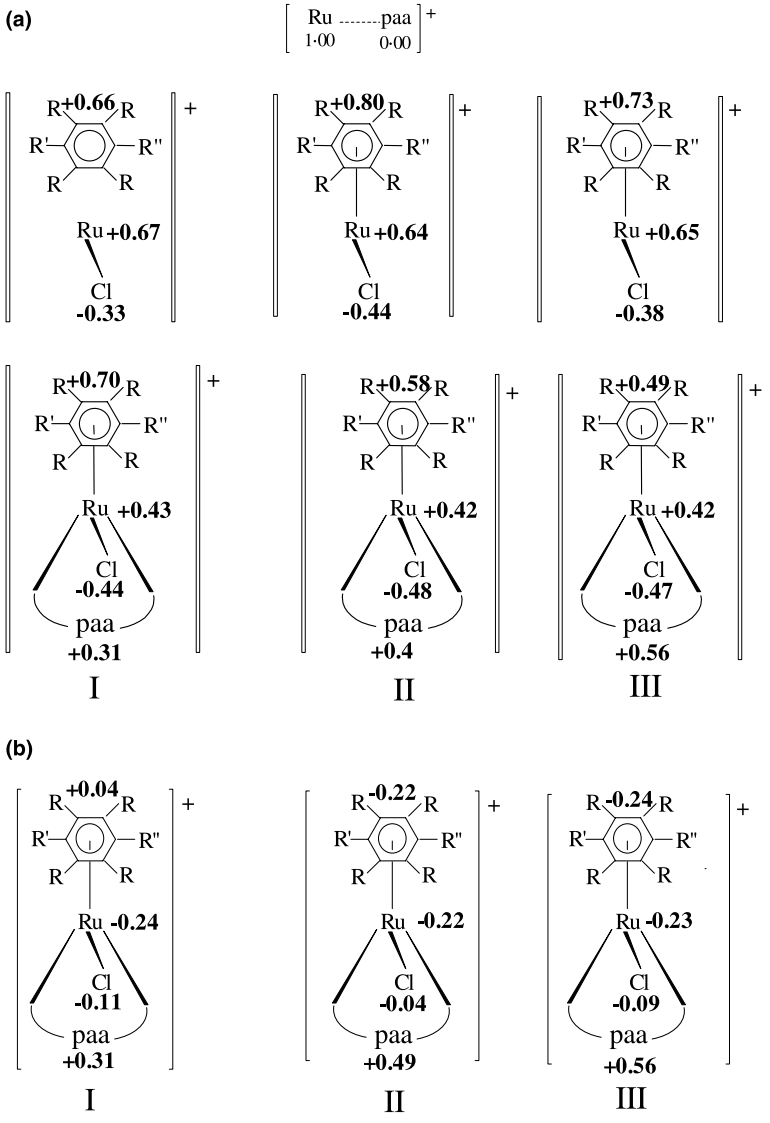

Fig. 6. (a) Calculated NBO charges of the complexes $[Ru(arene)Cl(paa)]^+$: arene = C_6H_6 (**I** R = R′ = R″ = H), C_6Me_6 (**II** R = R′ = R″ = Me), *p*-cymene (**III** R = H, R′ = CH_3, R″ = $CH(CH_3)_2$). (b) The changes caused by coordination of paa to $[Ru(arene)Cl(paa)]^+$: arene = C_6H_6 (**I** R = R′ = R″ = H), C_6Me_6 (**II** R = R′ = R″ = Me), *p*-cymene (**III** R = H, R′ = CH_3, R″ = $CH(CH_3)_2$).

3.2. Bonding analysis

The bonding energy, which is defined as a stabilization energy caused by coordination of paa ligand to $[(\eta^6\text{-arene})RuCl(paa)]^+$, associated with the reaction,

$$[(\eta^6\text{-arene})RuCl]^+ + [paa] \overset{BE}{\rightarrow} [(\eta^6\text{-arene})RuCl(paa)]^+ \quad (1)$$

Deformation energy, DEF (paa) is the energy required to restore the paa from the equilibrium structure to the structures adopted in the complex, and interaction energy, INT, is the stabilization energy resulting from the coordination of the distorted paa ligand to the $[(\eta^6\text{-arene})RuCl]^+$ fragments. Values of DEF for [paa] ligand are 4.66 kcal/mol in **I**, 5.80 kcal/mol in **II**, 9.92 kcal/mol in **III**. Values of INT are −96.41 kcal/mol for **I**, −85.25 kcal/mol for **II** and −94.23 kcal/mol for **III**. The most relevant information for the complexes **I**–**III** are the deformation energy of paa ligand and interaction energy resulting from the coordination of the distorted paa ligand to the $[(\eta^6\text{-arene})RuCl]^+$ fragments. It is very interesting to note that the paa ligand more strongly interacts with $[(\eta^6\text{-}C_{10}H_{14})RuCl]^+$ fragment than with $[(\eta^6\text{-}C_6Me_6)RuCl]^+$ and results greater DEF(paa) greater rotation about N2–N3 as well as about C1–C2 bonds Table 6 in **III** than in **II**. In the energy decomposition scheme, the bonding energy (BE) between $[(\eta^6\text{-arene})RuCl]^+$ and paa ligand is defined as [23]

$$BE = INT + DEF$$

Calculated values of the bonding energies for the three complexes containing paa ligand are reported in the Table 6.

Structurally characterized binuclear complexes resulting from the interaction of bridging ligands possessing N–N single bond, where rotation about N–N single bond is possible, are known mainly with the 3d transition metal ions. Only a couple of reports are known with 4d transition metal ions. In the present work, homo-nuclear bimetallic Ru(II) arene complexes in which, the metal ions are bridged by =N–N= moiety provided by the paa and =N–Ph–N= provided by pbp and =N–Ph–Ph–N= provided by bbp ligands are described. Although, both the ends in the ligands paa, pbp and bbp have got analogous donor sites, one can expect that in the complexes derived from paa, rotational freedom about N–N bond allows the ligand to adopt a *trans*, *cis* or in between twisted structures depending upon the co-ligands bound to the metal ion and their preference for different coordination geometries. Due to presence of phenyl spacers in the complexes derived from pbp or bbp such possibilities are weaker. To accommodate two metal centers in a stable complex the pyridyl rings twist away in the opposite directions. Structure of the representative mono and binuclear complexes $[(\eta^6\text{-}C_6Me_6)RuCl(paa)]BF_4$, $[\{(\eta^6\text{-}C_{10}H_{14})RuCl\}_2(\mu\text{-paa})](BF_4)_2$ and $[\{(\eta^6\text{-}C_{10}H_{14})RuCl\}_2(\mu\text{-pbp})](BF_4)_2$ has been confirmed by single crystal X-ray diffraction studies. These are the representative structures within the family of "piano stool" $[(\eta^6\text{-arene})RuCl]^+$ containing complexes with pyridyl-azine ligands. Presence of the $[(\eta^6\text{-arene})RuCl]$ moieties in the *trans* position supported by single crystal X-ray diffraction studies is in good agreement with this view point. We have presented the first theoretical study where the effects of arene ligands on bonding situations of pyridine-2-carbaldehyde azine (paa) in complexes $[(\eta^6\text{-arene})RuCl(paa)]^+$ (arene = C_6H_6, **I**; C_6Me_6, **II**; $C_{10}H_{14}$, **III**) are investigated at DFT/B3LYP. The calculated geometries are in excellent agreement with the experimental values. Geometrical parameters and bonding analysis reveal that *p*-cymene in complex **III** is relatively strongly bonded to ruthenium atom and, hence, strengthens the Ru–N1 and Ru–N2 bonds compared to those in **I** and **II**. We find greater deformation (variations in C1–N3–N2–C7 and N3–C1–C2–N4 in dihedral angles) of coordinated paa ligand in **III** from the equilibrium structure *trans*-paa. Smaller rotation about C1–C2 bond in **II** favours the formation of mononuclear complex and on the other hand, the greater rotation about N2–N3 as well as C1–C2 bonds in paa upon interaction with fragment $[(\eta^6\text{-}C_{10}H_{14})RuCl]^+$ favours the formation of a binuclear complex. There is direct relation between net positive charge on coordinated paa ligand and its deformation (variations in C1–N3–N2–C7 and N3–C1–C2–N4 in dihedral angles) from the equilibrium structure *trans*-paa.

Acknowledgements

Thanks are due to Council of Scientific and Industrial Research, New Delhi for providing financial assistance through the scheme [HRDG 01(1587)/99/EMR-II]. Two of the authors (A.S. and M.C.) acknowledges the receipt of SRF from C.S.I.R, New Delhi. We also thank The Head, SAIF, Central Drug Research Institute, Lucknow, for providing analytical and spectral facilities, and National Single Crystal X-ray Diffraction Laboratory, Indian Institute of Technology, Powai for X-Ray facilities. Special thanks are due to Prof. P. Mathur, Department of Chemistry, IIT, Mumbai for encouragements.

References

[1] (a) A. Juris, V. Balzani, F. Barigelletti, S. Campagna, P. Belser, A. Von Zelewsky, Coord. Chem. Rev. 84 (1988) 85;
(b) J.-M. Lehn, Supramolecular Chemistry, VCH, Weinheim, Germany, 1995;
(c) F. Bargiletti, L. Flamigni, Chem. Soc. Rev. 29 (2000) 1;
(d) J.K. Barton, A.T. Danishefksy, J.M. Goldberg, J. Am. Chem. Soc. 106 (1984) 2172;
(e) J. Kelly, A. Tossi, D. McConnel, C. Ohuigin, Nucleic Acids Res. 13 (1985) 6017;

(f) H. Brunner, R. Oeschey, B. Nuber, J. Chem. Soc., Dalton Trans. (1996) 1499;
(g) A. Frodl, D. Herebian, W.S. Sheldrick, J. Chem. Soc., Dalton Trans. (2002) 3664.
[2] (a) N. Gupta, N. Grover, G.A. Neyhart, P. Singh, H.H. Thorp, Inorg. Chem. 32 (1993) 310;
(b) C. Ceroni, F. Paolucci, S. Roffia, S. Serroni, S. Campagna, A.J. Bard, Inorg. Chem. 37 (1998) 2829;
(c) A. Klein, V. Kasack, R. Reinhardt, S. Torsten, T. Scheiring, S. Zalis, J. Fiedler, W. Kaim, J. Chem. Soc., Dalton trans. (1999) 575;
(d) N. Komatsuzaki, R. Katoh, Y. Himeda, H. Sugihara, H. Arakawa, K. Kasuga, J. Chem. Soc., Dalton Trans. (2000) 2053;
(e) C. Metcalfe, S. Spey, J.A. Thomas, J. Chem. Soc., Dalton trans. (2002) 4732;
(f) P.A. Anderson, F.R. Keene, T.J. Meyer, J.A. Moss, G.F. Strouse, J.A. Treadway, J. Chem. Soc., Dalton trans. (2002) 3820.
[3] (a) M. Ghedini, M. Longeri, F. Neve, J. Chem. Soc., Dalton Trans. (1986) 2669;
(b) Masa-Aki Haga K. Koizumi, Inorg. Chim. Acta 104 (1985) 47;
(c) J. Granifo, M.E. Vargas, E.S. Dodsworth, D.H. Farrar, S.S. Fielder, A.B.P. Lever, J. Chem. Soc., Dalton Trans. (1996) 4369;
(d) S. Gopinathan, S.A. Pardhy, C. Gopinathan, V.G. Puranik, S.S. Tavale, T.N.G. Row, Inorg. Chim. Acta 111 (1986) 133;
(e) M. Mikuriya, M. Fukuya, Chem. Lett. (1998) 421;
(f) Z. Xu, S. White, L.K. Thompson, D.O. Miller, M. Ohba, H. Okawa, C. Wilson, J.A.K. Howard, J. Chem. Soc., Dalton Trans. (2000) 1751;
(g) S. Pal, S. Pal, Inorg. Chem. 40 (2001) 4807.
[4] (a) W.J. Stratton, P.J. Ogren, Inorg. Chem. 9 (1970) 2588;
(b) W.J. Stratton, D.H. Busch, J. Am. Chem. Soc. 80 (1958) 1286;
(c) P.D.W. Boyd, M. Gerloch, G.M. Sheldrick, J. Chem. Soc., Dalton Trans. (1974) 1097;
(d) C.J. O'Connor, R.J. Romananch, D.M. Robertson, E.E. Eduok, F.R. Fronczek, Inorg. Chem. 22 (1983) 449.
[5] (a) M. Ghedini, A.M.M. Lanfredi, F. Neve, A. Tiripicchio, J. Chem. Soc., Chem Commun. (1987) 847;
(b) M. Ghedini, M. Longeri, F. Neve, A.M.M. Lanfredi, A. Tiripicchio, J. Chem. Soc., Dalton Trans. (1989) 1217.
[6] (a) A. Singh, A.N. Sahay, D.S. Pandey, J. Organomet. Chem. 642 (2002) 48;
(b) M. Chandra, A.N. Sahay, S.M. Mobin, D.S. Pandey, J. Organomet. Chem. 658 (2002) 43.
[7] (a) M.A. Bennett, A.K. Smith, J. Chem. Soc., Dalton Trans. (1974) 233;
(b) M.A. Bennett, T.N. Huang, T.W. Matheson, A.K. Smith, Inorg. Synth. 21 (1982) 74.
[8] (a) G.M. Sheldrick, SHELX 97, Program for Crystal Structure Determination, University of Gottingen, 1997;
(b) G.M. Sheldrick, SHELX 97, Program for Refinement of Crystal Structure, University of Gottingen, 1997;
(c) PLATON A.L. Spek, Acta Crystallogr., Sect. A 46 (1990) C31.
[9] A.D. Becke, J. Chem. Phys. 98 (1993) 5648.
[10] C. Lee, W. Yang, R.G. Parr, Phys. Rev. B 17 (1988) 785.
[11] (a) R. Krishnan, J.S. Binkley, R. Seeger, J.A. Pople, J. Chem. Phys. 72 (1980) 650;
(b) A.D. McClean, G.S. Chandler, J. Chem. Phys. 72 (1980) 5639.
[12] (a) P. Hay, W.R. Wadt, J. Chem. Phys. 82 (1985) 270;
(b) W.R. Wadt, P. Hay, J. Chem. Phys. 82 (1985) 284;
(c) P. Hay, W.R. Wadt, J. Chem. Phys. 82 (1985) 299.
[13] A.E. Reed, L.A. Curtiss, F. Weinhold, Chem. Rev. 88 (1988) 899.
[14] M.J. Frisch, G.W. Trucks, H.B. Schlegel, G.E. Scuseria, M.A. Robb, J.R. Cheeseman, V.G. Zakrzewski, J.A. Montgomery, Jr., R.E. Stratmann, J.C. Burant, S. Dapprich, J.M. Millam, A.D. Daniels, K.N. Kudin, M.C. Strain, O. Farkas, J. Tomasi, V. Barone, M. Cossi, R. Cammi, B. Mennucci, C. Pomelli, C. Adamo, S. Clifford, J. Ochterski, G.A. Petersson, P.Y. Ayala, Q. Cui, K. Morokuma, P. Salvador, J.J. Dannenberg, D.K. Malick, A.D. Rabuck, K. Raghavachari, J.B. Foresman, J. Cioslowski, J.V. Ortiz, A.G. Baboul, B.B. Stefanov, G. Liu, A. Liashenko, P. Piskorz, I. Komaromi, R. Gomperts, R.L. Martin, D.J. Fox, T. Keith, M.A. Al-Laham, C.Y. Peng, A. Nanayakkara, M. Challacombe, P.M.W. Gill, B. Johnson, W. Chen, M.W. Wong, J.L. Andres, C. Gonzalez, M. Head-Gordon, E.S. Replogle, J.A. Pople, GAUSSIAN 98 (Revision A.11), Gaussian Inc., Pittsburgh, PA, 2001.
[15] D.S. Pandey, R.L. Mishra, U.C. Agarwala, Ind. J. Chem. 31A (1991) 41.
[16] B. Gas, J. Klima, S. Zalis, A.A. Vecek, J. Electroanal. Chem. 222 (1987) 161.
[17] (a) V. Balzani, D.A. Bardwell, F. Barigelletti, R.L. Cleary, M. Guardigli, J.C. Jeffery, T. Sovrani, M.D. Ward, J. Chem. Soc., Daltons Trans. (1995) 3601;
(b) S. Campagna, G. Denti, G. De Rosa, L. Sabatino, M. Ciano, V. Balzani, Inorg. Chem. 28 (1989) 2565;
(c) C. Creutz, Prog. Inorg. Chem. 30 (1983) 1.
[18] (a) D. Braga, F. Grepioni, Chem. Commun. (1996) 571;
(b) D. Braga, F. Grepioni, G.R. Desiraju, J. Organomet. Chem. 548 (1997) 33;
(c) T. Steiner, Angew. Chem., Int. Ed. Engl 41 (2002) 48;
(d) G.R. Desiraju, T. Steiner, The Weak Hydrogen Bond in Structural Chemistry and Bfiology, Oxford University Press, Oxford, 1999;
(e) K. Ozeki, N. Sakabe, J. Tanaka, Acta Crystallogr., Sect. B 25 (1969) 1038.
[19] (a) S.F. Watkins, F.R. Fronczek, Acta Crystallogr., Sect. B 38 (1982) 270;
(b) F.B. McCormick, D.D. Cox, W.B. Gleason, Organometallics 6 (1993) 20;
(c) U. Beck, W. Hummel, H.B. Buergi, A. Ludi, Organometallics 6 (1993) 20;
(d) D.S. Pandey, A.N. Sahay, O.S. Sisodia, N.K. Jha, P. Sharma, H.E. Klaus, A. Cabrera, J. Organomet. Chem. 592 (1999) 278.
[20] (a) M.I. Bruce, F.S. Wong, B.W. Skelton, A.H. White, J. Chem. Soc., Dalton Trans. (1981) 1398;
(b) J.M. Clear, C.M. O'Connell, J.G. Vos, C.J. Cardin, A.J. Edwards, J. Chem. Soc., Chem. Commun. (1980) 750;
(c) R.O. Gould, C.L. Jones, R.D. Robertson, T.A. Stephenson, J. Chem. Soc., Dalton Trans. (1981) 129.
[21] (a) N.T. Huang, W.T. Pennington, J.N. Petersen, Acta Crystallogr., Sect. C 47 (1991) 2011;
(b) A. Escuer, R. Vicente, T. Comas, J. Ribas, M. Gomez, X. Solans, D. Gatteschi, C. Zanchini, Inorg. Chim. Acta 181 (1991) 51;
(c) W.S. Sheldrick, H.S. Hagen-Eckhard, S. Heeb, Inorg. Chim. Acta 206 (1993) 15;
(d) W. Luginbuehl, P. Zbinden, P.A. Pittet, T. Armbruster, H.B. Buergi, A.E. Merbach, A. Ludi, Inorg. Chem. 30 (1991) 2350;
(e) A.J. Davenport, D.L. Davies, J. Fawcett, S.A. Garratt, D.R. Russell, J. Chem. Soc., Dalton Trans. (2000) 4432.
[22] K.A. Wiberg, Tetrahedron 24 (1991) 1083.
[23] (a) K. Morokuma, J. Chem. Phys. 55 (1971) 1236;
(b) K. Morokuma, Acc. Chem. Res. 10 (1977) 294.